

# FlexTSF: A Flexible Forecasting Model for Time Series with Variable Regularities

Jingge Xiao  
xiao@L3S.de  
L3S Research Center  
Leibniz University Hannover  
Germany

Yile Chen  
yile001@e.ntu.edu.sg  
Nanyang Technological University  
Singapore

Gao Cong  
gaocong@ntu.edu.sg  
Nanyang Technological University  
Singapore

Wolfgang Nejdl  
nejdl@L3S.de  
L3S Research Center  
Leibniz University Hannover  
Germany

Simon Gottschalk  
gottschalk@L3S.de  
L3S Research Center  
Leibniz University Hannover  
Germany

## Abstract

Forecasting time series with irregular temporal structures remains challenging for universal pre-trained models. Existing approaches often assume regular sampling or depend heavily on imputation, limiting their applicability in real-world scenarios where irregularities are prevalent due to diverse sensing devices and recording practices. We introduce FlexTSF, a flexible forecasting model specifically designed for time series data with variable temporal regularities. At its foundation lies the IVP Patcher, a continuous-time patching module leveraging Initial Value Problems (IVPs) to inherently support uneven time intervals, variable sequence lengths, and missing values. FlexTSF employs a decoder-only architecture that integrates normalized timestamp inputs and domain-specific statistics through a specialized causal self-attention mechanism, enabling adaptability across domains. Extensive experiments on 16 datasets demonstrate FlexTSF’s effectiveness, significantly outperforming existing models in classic forecasting scenarios, zero-shot generalization, and low-resource fine-tuning conditions. Ablation studies confirm the contributions of each design component and the advantage of not relying on predefined fixed patch lengths.

## CCS Concepts

- Computing methodologies → Neural networks; • Mathematics of computing → Time series analysis; • Information systems → Data mining.

## Keywords

time series forecasting, temporal irregularity, IVP Patcher

## 1 Introduction

Time series forecasting, the task of predicting future values based on historical observations, plays an indispensable role across numerous domains, including finance, retail, healthcare, and meteorology [17, 28]. Recently, there has been significant research on universal time series forecasting models, which can be directly applied to various domains after pre-training [1, 38, 52]. However, alongside broader applications, a key challenge arises: **temporal irregularity**—the existence of missing values, uneven time intervals, and variable sequence lengths.

We illustrate temporal irregularity in Figure 1. (a) shows regularly sampled data; (b) depicts missing data due to events like holidays; (c) presents blood pressure measurements becoming denser as a patient’s condition worsens; (d) shows irregular satellite observations influenced by atmospheric conditions such as clouds and fog; and (e) illustrates irregular temporal distributions. The temporal irregularity exists not only in input data. From the output perspective, users sometimes need forecasts only around specific time points. For instance, diabetic patients typically focus on glucose levels before and after meals, rather than tracking them for all 1,440 minutes of a day. Weather forecasts may alternate between long-term daily predictions and imminent rainfall probabilities. To cover all time points, a forecasting model designed for regular time series has to operate at the finest granularity, leading to unnecessarily long prediction sequences (e.g., 14,400 minutes for ten days). Moreover, whether in pre-training or downstream applications, the wide range of measurement types (electricity consumption, exchange rates, systolic blood pressure, etc.) comes with diverse temporal granularities (e.g., minutes, hours, days, etc.), complicating universal generalization for a single model.

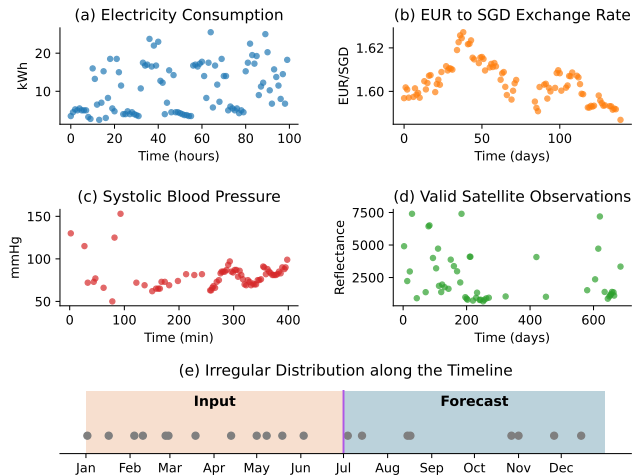


Figure 1: Illustrations of temporal irregularity.

In this paper, we propose FlexTSF<sup>1</sup>, a flexible time series forecasting model that not only performs well on data with temporal irregularity but is also broadly applicable across domains with various temporal granularities. FlexTSF employs a decoder-only architecture, where time series input data is organized into patches. Previously observed patches attend to the generation of future patches, which are then transformed into forecasts. Built on this backbone, FlexTSF introduces a novel patching module and a domain self-adaptation mechanism.

Specifically, FlexTSF incorporates IVP Patcher, a continuous-time patching module that inherently supports learning representations for time series patches exhibiting the aforementioned temporal irregularities. Classic patching methods organize data points within fixed-size windows to form input units for the model [19, 35]. They assume uniform temporal distribution—an assumption that holds mainly for regular, well-structured time series [15, 52]. Alternatively, IVP Patcher learns representations by solving Initial Value Problems (IVPs) [4], leveraging differential equations to model temporal dynamics across arbitrary time intervals within each patch. It removes the reliance on rigid temporal regularity and enables the model to operate directly on data with missing values and uneven time intervals—without imputation. Moreover, IVP Patcher eliminates the need to predefined a fixed patch size as a hyperparameter, allowing the model to automatically select or dynamically learn a suitable patch size based on data characteristics. This enhances modeling flexibility and reduces manual tuning effort.

Moreover, FlexTSF addresses diverse temporal granularities by transforming time information from any domain into a unified form. Instead of manually specifying structured temporal information (e.g., years or seconds), FlexTSF normalizes observation timestamps and conditions the generation process on statistics derived during data normalization via causal self-attention. A special computing node, placed at the forefront of FlexTSF’s decoder-only architecture, ingests static domain-specific features and guides the generation process, enabling self-adaptation across domains.

Our evaluation on 16 benchmark datasets demonstrates that FlexTSF achieves the lowest MSE in 22 of 24 irregular-forecasting tasks (8 datasets  $\times$  3 horizons), exhibits better robustness across varying missing rates, and significantly outperforms state-of-the-art baselines in the zero-shot setting. Ablations further confirm the contribution of each component and the benefits of using random patch lengths.

We summarize our main contributions as follows:

- We propose FlexTSF, to our knowledge the first universal forecasting model built from the perspective of breaking data regularity constraints.
- We introduce IVP Patcher, a continuous-time patching module, to handle irregular time series, overcoming limitations of traditional fixed-size patching methods.
- We propose a timestamp normalization scheme and a forefront computing node, enabling domain-aware adaptation and improving cross-domain generalization.
- We conduct extensive evaluations demonstrating FlexTSF’s superior forecasting capability in classic, zero-shot, and low-resource fine-tuning scenarios, supported by ablation studies.

<sup>1</sup>Source code is available at <https://anonymous.4open.science/r/FlexTSF-C3AE>.

## 2 Related Work

*Universal Time Series Forecasting Models.* There is an emerging trend of research training universal forecasting models from scratch using time series. In Table 1, we provide a technical comparison of six open-source models [14, 15, 18, 30, 33, 38] with FlexTSF. All these models are trained on large collections of time series data and support zero-shot prediction on new datasets. Most of these models are designed for well-structured and regularly sampled time series [57], leaving them ill-equipped to handle the heterogeneous data structure issues often encountered in real-world scenarios. Darlow et al. [14] considered irregularity when building the model, but the model was not applied to irregular time series forecasting. In contrast, FlexTSF stands out by effectively handling various time series characteristics, such as missing values, varying lengths, and irregular intervals, making it more adaptable to diverse applications.

*Irregular Time Series Modeling.* Irregular time series are becoming increasingly prevalent due to widespread adoption of various sensing devices and recording practices [51]. In recent years, substantial progress has been made in developing models to handle irregular time series, as demonstrated by works such as GRU-D [10], Latent-ODE [39], mTAN [44], CRU [42], ContiFormer [13], and t-PatchGNN [59]. However, none of them succeeded to build and pre-train a universal time series forecasting model that is broadly applicable to various domain and regularities without post-training.

More related works are discussed in Appendix A.1.

## 3 Problem Formulation & Prerequisites

*Problem Formulation.* We consider a time series  $S$  as a sequence of  $M$  elements  $S = \{(\mathbf{x}_i, t_i)\}_{i=1}^M$ , where each element  $(\mathbf{x}_i, t_i)$  consists of an observation  $\mathbf{x}_i$  collected at timestamp  $t_i$ . This formulation is flexible to accommodate a diverse range of time series characterized by different sequence lengths (varying  $M$  across samples), irregular time intervals ( $t_{i+1} - t_i \neq t_i - t_{i-1}$ ), and incomplete observations (missing variables in  $\mathbf{x}_i$ ). Referencing previous works [14, 35, 63], we address multivariate time series in a channel-independent manner. Our goal is to develop a universal forecasting model that takes any time series  $S$  as input and predict its future values  $\{\mathbf{x}_i\}_{i=M+1}^{M+H}$  over a subsequent time window  $\{t_i\}_{i=M+1}^{M+H}$ , where  $H$  denotes the forecast horizon. Notation is summarized in Appendix A.2.

*Patching.* Patching is a common strategy to obtain time series representations by organizing data sequence into fixed-length segments, facilitating efficient modeling with transformers [15, 35]. Given a time series, a patch  $V$  is typically defined as a subsequence  $V = \{(\mathbf{x}_i, t_i)\}_{i=p_s}^{p_e}$ , where  $p_s$  and  $p_e$  denote the starting and ending indices of the patch, respectively. Each patch aggregates a consecutive segment of length  $p = p_e + 1 - p_s$  and serves as a modeling unit. Classic patching methods use a predefined fixed  $p$  for each dataset, often requiring careful tuning for optimal performance.

*Initial Value Problems.* An initial value problem (IVP) [41] models the evolution of a system’s state by solving an ordinary differential equation (ODE) of the form  $\frac{dz(t)}{dt} = f(t, z(t))$ , with initial condition  $z(t_0) = z_0$ , where  $z(t)$  denotes the latent state at time  $t$ ,  $f$  describes the system’s time-dependent dynamics, and  $z_0$  is the initial latent state at  $t_0$ . Two characteristics of IVPs make them suitable

**Table 1: Comparison between pre-trained time series forecasting models. "TV" indicates time-value pairs. ✓(or ✗) indicates the model (does not) naturally support this kind of data characteristic.**

	ForecastPFN	Lag-Llama	DAM	TimesFM	MOIRAI-MoE	Sundial	FlexTSF
<b>Tokenization</b>	Point-wise TV	Lag Feature	Point-wise TV	Patch	Patch	Patch	IVP Patcher
<b>Architecture</b>	Encoder-Only	Decoder-Only	Encoder-Only	Decoder-Only	Encoder-Only	Decoder-Only	Decoder-Only
<b>Forecast</b>	Time Query	Autoregression	Basis Functions	Autoregression	Masked Prediction	Autoregression	Masked Autoregression
<b>Variate</b>	Univariate	Univariate	Univariate	Univariate	Multi/Univariate	Univariate	Univariate
<b>Probabilistic</b>	✗	✓	✗	✗	✓	✓	✓
<b>Missing Values</b>	✗	✗	✓	✗	✗	✗	✓
<b>Various Length</b>	✓	✓	✓	✓	✗	✓	✓
<b>Irregular Interval</b>	✓	✗	✓	✗	✗	✗	✓

for patching irregular time series: 1) The derivative  $f$  naturally accommodates data with irregular temporal distributions. 2)  $f(t, z(t))$  is capable of modeling time-dependent dynamics, which is ideal for time series that are often driven by internal or external factors varying over time (complex, non-stationary behaviors). Pioneering works such as Neural ODEs [12] and Neural Flows [4] provided fundamental tools for learning continuous-time, time-dependent dynamics from irregularly sampled time series.

*Value Normalization.* Recent research in time series forecasting often adopts a two-step normalization scheme for input values: global and instance normalization. Given a value sequence  $X = \{\mathbf{x}_i\}_{i=1}^M$  from dataset  $D$ , global normalization computes the mean  $\mu_g$  and standard deviation  $\sigma_g$  over  $D$ , then standardizes each value. Instance normalization  $G_i$  [35] further standardizes each sequence using its own mean  $\mu_i$  and standard deviation  $\sigma_i$ . Formally:  $X' = G_i(G_g(X))$ , yielding normalized values  $X'$ . While value normalization is extensively applied, normalization of temporal information remains largely overlooked.

## 4 Methodology

### 4.1 Overview

An overview of FlexTSF’s dataflow is illustrated in Figure 2(a). FlexTSF begins by applying value and time normalization to the raw input sequence, bringing observations into a unified numeric and temporal scale. The normalized series is then split into patches, with dummy patches appended at the end to represent the forecast target timestamps. Each patch is processed by the encoder part of the IVP Patcher to create a latent state anchor  $z_0$ , which is used in two parallel ways: it is evolved forward in time by the decoder part of the IVP Patcher to reconstruct the patch, and also delivered as a patch-level embedding to a causal self-attention module.

The self-attention stack processes the sequence of patch representations, along with static features provided by a Leader node and time embeddings applied at each attention layer. After the attention stack, hidden states of dummy patches are used as forecast anchors, which are passed to the decoder part of the IVP Patcher to generate forecasts by evolving forward to target timestamps. The model is trained end-to-end using a combination of patch-level ELBO and forecast log-likelihood losses, with the IVP Patcher focused on learning local dynamics and the attention module capturing higher-level temporal dependencies across patches. We detail different components in the following.

### 4.2 IVP Patcher

The IVP Patcher is a module designed to handle temporal irregularity by replacing fixed-size patching with a continuous-time formulation. As shown in Figure 2(c), it treats values in each patch as indirect observations (blue dots) of underlying continuous latent processes (green lines) governed by ODEs. This contrasts with classic patching (Figure 2(d)), which extracts and transforms fixed-size value sequences while ignoring time information. IVP Patcher consists of two parts, and its procedure is outlined in Algorithm 1.

---

#### Algorithm 1 IVP Patcher

---

**Part 1:** Generating Representations through Solving IVPs

Backward in Time

**Input:** One Patch  $V = \{(\mathbf{x}_i, t_i)\}_{i=1}^p$

**Output:** Patch Representation  $\mathbf{r}$

- 1:  $\{z_i\}_{i=1}^p = \text{Linear}(\{\mathbf{x}_i\}_{i=1}^p)$
- 2:  $\{z_{0,i}\}_{i=1}^p = \{\text{IVPSolve}(z_i, t_i, t_1)\}_{i=1}^p$
- 3:  $q_\phi(z_0|V) = \text{Inference}(\{z_{0,i}\}_{i=1}^p)$
- 4:  $\mathbf{r} \sim q_\phi(z_0|V)$
- 5: **return**  $\mathbf{r}$

---

**Part 2:** Making Forecasts through Solving IVPs Forward in Time

**Input:** Predicted Representation  $\hat{\mathbf{r}}$

**Output:** One Patch Forecasts  $\{\hat{\mathbf{x}}_i\}_{i=p_s}^{p_e}$

- 1:  $z_{p_s} = \hat{\mathbf{r}}$
- 2:  $\{z_i\}_{i=p_s}^{p_e} = \{\text{IVPSolve}(z_{p_s}, t_{p_s}, t_i)\}_{i=p_s}^{p_e}$
- 3:  $\{\hat{\mathbf{x}}_i\}_{i=p_s}^{p_e} = \text{Linear}(\{z_i\}_{i=p_s}^{p_e})$
- 4: **return**  $\{\hat{\mathbf{x}}_i\}_{i=p_s}^{p_e}$

---

#### 4.2.1 Generating Representations through Backward IVP Solving.

For each input patch, a linear layer first maps each observed data point  $\mathbf{x}_i$  to an initial latent state  $z_i$ . To capture the temporal dynamics within the patch and establish a unified representation, we employ an IVP solver to evolve these latent states backward in time to the starting timestamp of the patch (denoted as  $t_1$  for simplicity in Algorithm 1 when  $p_s = 1$ ). Specifically, for each data point  $(\mathbf{x}_i, t_i)$ , the corresponding latent state  $z_i$  serves as the initial condition at time  $t_i$ , and the IVP solver computes latent state  $z_{0,i}$  at reference time  $t_1$  by integrating backward over the time difference

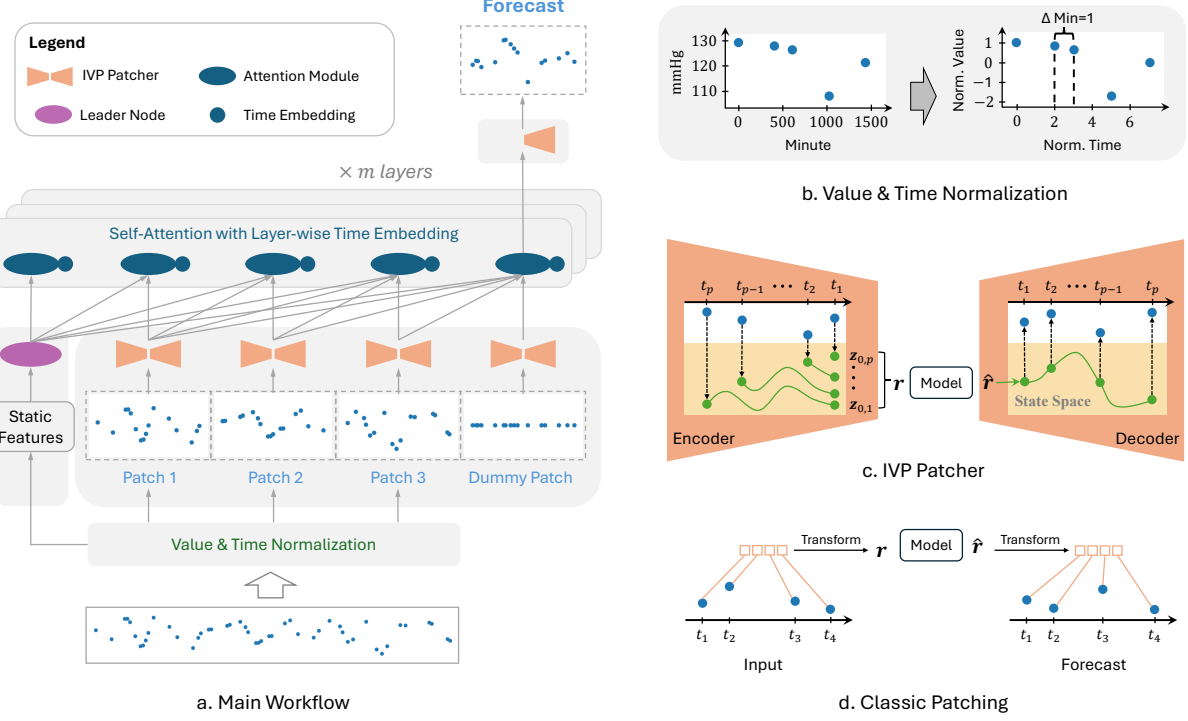


**Figure 2: Framework Overview.** (a) FlexTSF normalizes input time series, extracts patch representations via the IVP Patcher, applies self-attention with a Leader node, and decodes dummy patches to forecasts. (b) A time series with irregular intervals is transformed into a numerical scale with the minimum interval equal to 1. (c) IVP Patcher models continuous-time dynamics on irregular data by solving IVPs. (d) Classic patching directly transforms fixed-size sequences while ignoring time information.

$\Delta t_i = t_1 - t_i$ . This backward evolution allows aggregating information from different time points to a common temporal reference. It is simultaneously applied to all data points within the patch.

To obtain a generalizable patch representation  $\mathbf{r}$ , we draw inspiration from the Variational Autoencoder (VAE) framework [23] to learn a latent distribution that encapsulates the essential information within the patch. Given evolved latent states  $\{z_{0,i}\}_{i=1}^p$ , we infer a variational posterior distribution  $q_\phi(z_0|V)$ , which approximates the intractable true posterior. The Inference function models this posterior as a mixture of diagonal Gaussian distributions:

$$q_\phi(z_0|V) = \sum_{i=1}^p \pi_i \mathcal{N}(z_0|\mu_{z_{0,i}}, \sigma_{z_{0,i}}^2), \quad (1)$$

where  $\{\pi_i\}_{i=1}^p$  are the mixing coefficients for  $p$  components, with

$$\pi_i = \frac{1/\text{KL}_i}{\sum_j 1/\text{KL}_j + \epsilon}, \quad (2)$$

where  $\text{KL}_i = \text{KL}[\mathcal{N}(\mu_{z_{0,i}}, \sigma_{z_{0,i}}^2) \parallel \mathcal{N}(\mathbf{0}, \mathbf{I})]$ .

To sample the final patch representation  $\mathbf{r}$ , we independently draw  $\tilde{z}_{0,i} \sim \mathcal{N}(\mu_{z_{0,i}}, \sigma_{z_{0,i}}^2)$  and compute a KL-weighted average:  $\mathbf{r} = \sum_{i=1}^p \pi_i \cdot \tilde{z}_{0,i}$ . This approximates the mixture's mean—while emphasizing higher-information components—and yields a more

concentrated, low-variance latent:

$$\mathbf{r} \sim \mathcal{N}\left(\sum_i \pi_i \mu_{z_{0,i}}, \sum_i \pi_i^2 \sigma_{z_{0,i}}^2\right), \quad (3)$$

where each component's mean  $\mu_{z_{0,i}}$  and standard deviation  $\sigma_{z_{0,i}}$  are parameterized by neural networks conditioned on the patch.

**4.2.2 Making Forecasts through Forward IVP Solving.** To generate forecasts for future timestamps, we leverage the latent representation  $\hat{\mathbf{r}}$  produced by the attention module. It is treated as the initial condition  $z_{p_s} = \hat{\mathbf{r}}$  at starting time  $t_{p_s}$  of the forecast horizon. We then employ the IVP Patcher to evolve this latent state forward in time to desired future timestamps  $\{t_i\}_{i=p_s}^{p_e}$ . For each future timestamp  $t_i$ , the IVP solver computes the corresponding latent state  $z_i$  by integrating forward over time difference  $\Delta t_i = t_i - t_{p_s}$ . The evolution to all future timestamps within a forecast patch is also done simultaneously, as the computation of state  $z_i$  at a specific time  $t_i$  only depends on the initial state  $z_{p_s}$ , which is same for timestamps within a patch. Finally, a linear layer maps these future latent states  $\{z_i\}_{i=p_s}^{p_e}$  to the predicted values  $\{\hat{x}_i\}_{i=p_s}^{p_e}$ . These values parameterize an isotropic Gaussian likelihood  $p_\theta(V|z_0) = \prod_{i=p_s}^{p_e} \mathcal{N}(x_i | \hat{x}_i, \sigma^2 \mathbf{I})$ , which is used in the reconstruction term of the patch loss.

The patch loss balances reconstruction and regularization:

$$\mathcal{L}_{\text{patch}}(V) = \underbrace{\frac{1}{p} \sum_{i=1}^p \text{KL}_i}_{\text{KL Regularization}} + \underbrace{\beta \cdot \mathbb{E}_{q_\phi} [-\log p_\theta(V | z_0)]}_{\text{Reconstruction}}, \quad (4)$$

where  $\beta$  controls the trade-off.

**4.2.3 Integration with the Attention Module.** In essence, the IVP Patcher acts as a patch-level variational autoencoder: the encoder solves backward IVPs on raw point-level inputs to produce a latent representation  $\mathbf{r}$ , which is used both to reconstruct the original patch (yielding the ELBO loss) and as input to the attention module. Once the attention stack predicts the next patch embedding  $\hat{\mathbf{r}}$ , the decoder reuses IVP solving—now forward in time—to generate concrete forecast values. To preserve the temporal context of each patch, we assign its first timestamp as a time identifier  $\tau_k$  for patch  $k$ . When solving IVPs backward in time, all latent states within a patch are aligned to  $\tau_k$ , and when forward in time, forecasts originate from  $\tau_k$ , ensuring the model remains aware of each patch's position in the overall sequence.

**4.2.4 Patch Length.** The IVP Patcher offers the advantage of dynamically selecting patch lengths for each input. We propose two strategies for generating patch lengths: deterministic and random. The deterministic approach determines the patch length based on specific input characteristics, such as sequence length, allowing inputs with different properties to be processed using corresponding patch lengths. This addresses the limitation of using a single fixed patch length for pretraining models on heterogeneous datasets [38, 52].

The random approach independently samples a patch length  $p$  from a candidate pool  $\mathcal{P}$  for each input. During training, we track the cumulative forecasting loss and usage count of each  $p$  over a validation epoch. Patch lengths with consistently poor performance—quantified via z-scores exceeding a threshold—are pruned from  $\mathcal{P}$ . The remaining lengths are reweighted with the cumulative loss. This process gradually concentrates computation on lengths that empirically yield better predictions. Once the pool has been refined and the importance weights  $w_p$  are normalized, the model obtains a forecast in one of two ways: (1) by selecting the best-performing length  $p^* = \arg \max_{p \in \mathcal{P}} w_p$  and using its prediction  $\hat{X}^+ = \hat{X}_{p^*}^+$ , or (2) by computing a weighted ensemble forecast  $\hat{X}^+ = \sum_{p \in \mathcal{P}} w_p \hat{X}_p^+$ . This approach is intended to minimize manual hyperparameter tuning and leverage patches of varying sizes to capture composite temporal patterns.

### 4.3 Time Normalization & Domain Adaptation

In addition to value normalization, we propose a time normalization scheme to mitigate the impact of diverse temporal granularities. Given a sequence of timestamps  $T = \{t_i\}_{i=1}^M$  associated with a sample  $\mathcal{X}$  from dataset  $D$ , we define a dataset-level time unit  $\omega_g$  as the reciprocal of the sampling frequency in  $D$ . For each instance, we compute the time differences  $\{\Delta t_i = t_{i+1} - t_i\}_{i=1}^{M-1}$  and define the minimum interval as the instance-level unit  $\omega_i = \min_i \Delta t_i$ . Each interval is then scaled as  $\Delta t'_i = \Delta t_i / \omega_i$ , and the normalized timestamps are computed by  $t'_i = t_1 + \sum_{j=1}^{i-1} \Delta t'_j$ . After normalization,

the smallest time interval is scaled to 1 (Figure 2(b)), and other intervals are multiples of the smallest. This produces unitless time indicators  $T' = \{t'_i\}_{i=1}^M$  to unify different temporal granularities and irregularities. The time units are reserved for the next step.

To enable the model to self-adapt to diverse domains, we use the value normalization plus time normalization strategy to decouple static domain information from dynamic temporal patterns. Instead of leaving these statistics aside and using them to "de-normalize" output values of the forecasting model [34, 50], we concatenate the statistics into a feature vector  $L = [\mu_g, \sigma_g, \mu_i, \sigma_i, \omega_g, \omega_i]$ , and add an extra computation node at the forefront of the causal self-attention (Figure 2(a)), referred to as Leader node, which disseminates information to all subsequent nodes based on the attention's look-backward architecture. These six features are chosen as they are ubiquitous and can be obtained from any dataset. To integrate information, we append dummy patches to the end of the patch sequence as forecast placeholders, initialized with the input mean.

To enhance the self-attention mechanism's capability in capturing ordering and temporal information, we apply layer-wise time embedding, thereby eliminating the need for input position embeddings. As self-attention has been found to be less effective in capturing temporal order of time series [22, 58], we incorporate rotary position embedding (RoPE) [45] to embed the time indicator  $\tau$  of each patch. Note that  $\{\tau_k\}_{k=0}^K$  may exhibit variable intervals as the raw input time series can be irregular. Additional details of the attention module can be found in the Appendix A.3.

### 4.4 Training Objective

After the attention stack, each dummy patch's hidden state is passed to the shared IVP Patcher's decoder to generate forecasts  $\{\hat{\mathbf{x}}_{M+h}\}_{h=1}^H$  at timestamps  $\{t_{M+h}\}_{h=1}^H$ . Following the autoregressive chain rule, we adopt the assumption that future steps are conditionally independent given the past and their own time-stamps [43, 52]:

$$\begin{aligned} p(\mathbf{x}_{>M} | \mathbf{x}_{\leq M}, t_{>M}) &= \prod_{h=1}^H p(\mathbf{x}_{M+h} | \mathbf{x}_{\leq M}, \mathbf{x}_{M+1:M+h-1}, t_{M+h}) \\ &\approx \prod_{h=1}^H p(\mathbf{x}_{M+h} | \mathbf{x}_{\leq M}, t_{M+h}). \end{aligned} \quad (5)$$

This formulation removes teacher forcing, prevents error accumulation, and enables a single forward pass for all horizons. The forecast loss is defined as the sum of negative Gaussian log-likelihoods with fixed variance  $\sigma^2$  [4, 12]:

$$\mathcal{L}_{\text{forecast}} = - \sum_{h=1}^H \log \mathcal{N}(\mathbf{x}_{M+h} | \hat{\mathbf{x}}_{M+h}, \sigma^2 \mathbf{I}). \quad (6)$$

FlexTSF is trained end-to-end by optimizing a joint objective unifying patch-level representation learning (Section 4.2.2) with multi-horizon forecasting:

$$\mathcal{L} = \lambda \frac{1}{K} \sum_{k=1}^K \mathcal{L}_{\text{patch}}(V) + \mathcal{L}_{\text{forecast}}, \quad (7)$$

with  $\lambda$  balancing the two objectives. The model can be trained in both supervised and self-supervised settings. An illustration can be found in Appendix A.4.

## 5 Experiments

### 5.1 Experimental Setups

We evaluate FlexTSF across different domains and training setups using two non-overlapping groups of datasets: pre-training datasets  $\mathcal{D}_p$  and held-out datasets  $\mathcal{D}_h$ . We conduct three stages of experiments: (i) time series forecasting using standard training-validation-testing splits on  $\mathcal{D}_h$ ; (ii) zero-shot forecasting on the test partition of  $\mathcal{D}_h$  with a model pre-trained on  $\mathcal{D}_p$  (63 million parameters); and (iii) low-resource fine-tuning on  $\mathcal{D}_h$  using a limited number of samples (e.g., 50, 100, 150).

**5.1.1 Datasets.** Our pre-training group  $\mathcal{D}_p$  comprises 2.4 M sequences (lengths 18–1024) from Monash [20] and UCR&UEA [2, 3, 16], covering domains such as tourism, banking, climate and health. The held-out group  $\mathcal{D}_h$  contains datasets from the Long Time Series Forecasting Benchmark [25, 53] and the Irregular Time Series Benchmark [27, 39]. After removing overlaps with  $\mathcal{D}_p$ ,  $\mathcal{D}_h$  contains 8 datasets with regular time series and 8 datasets with time series of different irregularities. Table 2 lists all datasets along with the types of temporal irregularity they exhibit. Each dataset in  $\mathcal{D}_h$  is split into training, validation, and testing sets, following their original splits if known or a split ratio of 8:1:1, otherwise. Further details on the datasets can be found in Appendix A.6.

**Table 2: Held-out datasets. (1)–(3) denote types of temporal irregularity: (1) missing values, (2) varying sequence lengths, (3) unequal time intervals. “+” indicates multiple types.**

Category	Datasets
Regular time series	ETTh1, ETTh2, ETTm1, ETTm2, ExRate, Illness, Weather, Electricity
Irregular time series	
• (1) + (2)	MetrLA, ArabDigit, CharTraj
• (1) + (3)	HAR
• (2) + (3)	SaTSM
• (1) + (2) + (3)	eICU, Physio12, MIMIC4

**5.1.2 Baselines.** We incorporate a comprehensive set of baselines spanning three categories: (1) **Regular**: models assuming uniformly spaced and complete time series, including DLinear [58], NHiTS [9], PatchTST [35], iTransformer [31], and TimeMixer [49]; (2) **Irregular**: models explicitly handling temporal irregularities, including mTAN [44], Latent-Flow [4], CRU [42], ContiFormer [13], IVP-VAE [54], and t-PatchGNN [59]; and (3) **Zero-shot**: universal forecasters pre-trained on large corpora, including Lag-Llama [38], TimesFM [15], MOIRAI-MoE [30], Sundial [33], and also statistical model ARIMA [7] as a reference. Since baselines designed for regular time series and zero-shot forecasting do not natively support irregular data, we adapt them by imputing missing values using the mean of each time series.

**5.1.3 Implementation Details.** For regular datasets, we use a fixed input length of 96 and a forecasting horizon of 96. For irregular datasets, it is impractical to define fixed input and output lengths across all cases. Instead, we adopt a forecast-to-input ratio  $H/M$

and vary it across  $\{0.25, 0.5, 1.0\}$  to evaluate performance under different forecasting horizons.

The pre-trained FlexTSF model consists of 6 attention layers, each with 12 self-attention heads and a hidden size of 768, for a total of 63 million parameters. In the IVP Patcher, we employ ResNetFlow [4] to solve initial value problems. Regarding patch length, we used the random approach (See Section 4.2.4) in classic training and the deterministic approach in pre-training, zero-shot and fine-tuning. The Leader node of FlexTSF is implemented as a multilayer perceptron. We set the loss function coefficients to  $\lambda = 0.1$  and  $\beta = 1.0$ . Additional hyperparameter settings are provided in Appendix A.5.

Following prior work [1, 35, 44], each experiment is repeated three times with different random seeds for dataset splitting and parameter initialization. Model performance is reported as the mean and standard deviation of Mean Squared Error (MSE). All models are evaluated under the same computing environment with NVIDIA V100 GPUs for classic training, and H100 GPUs for pre-training and inference.

### 5.2 Time Series Forecasting

Table 3 presents the results in the classic training-validation-testing setting on held-out irregular time series datasets. FlexTSF consistently outperforms other models in 22 of 24 cases (8 datasets  $\times$  3 horizons), demonstrating its effectiveness in capturing temporal dynamics and dealing with irregularities. Among the baselines, some methods originally designed for regular time series achieve decent results on irregular datasets, while those tailored for irregular time series perform particularly well on datasets characterized by higher rates of missing data and greater sparsity, such as eICU, Physio12 and MIMIC4.

Figure 3 further investigates the impact of various missing rates on the forecasting performance of four representative models. As expected, model performance degrades (higher MSE) as the missing rate increases. However, FlexTSF consistently exhibits superior robustness, maintaining a relatively lower MSE across missing rates and datasets, highlighting its effectiveness in handling irregular data. The MSE of models like PatchTST and TimeMixer initially rises and then decreases at very high missing rates. This behavior occurs because, at high missing rates, models may shift focus to the remaining patterns, and heavy imputation can smooth out noisy fluctuations they might otherwise overfit to.

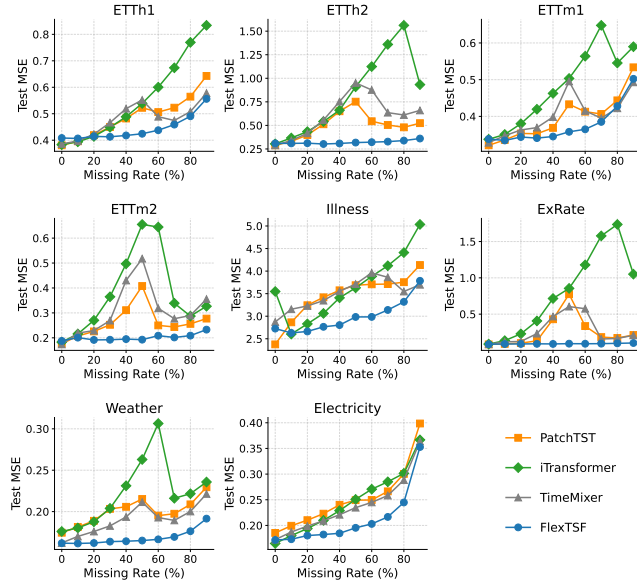
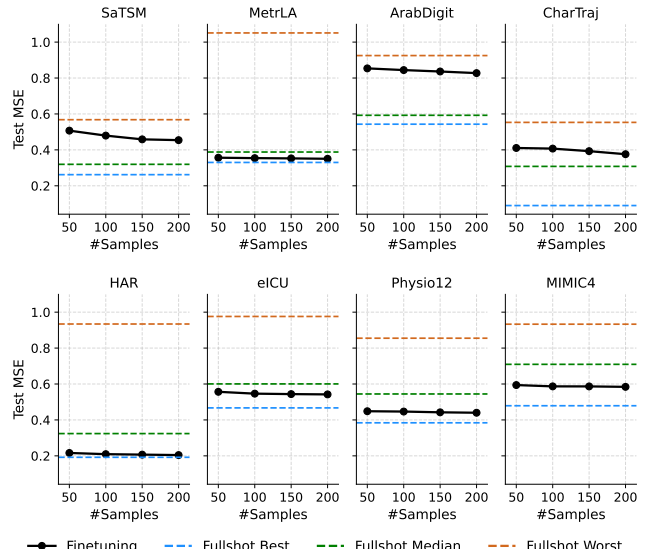
### 5.3 Zero-shot and Low-resource Fine-tuning

Table 4 shows the results of our zero-shot experiments, where we pre-train FlexTSF on  $\mathcal{D}_p$  and then directly apply it to the test sets of held-out irregular time series datasets. FlexTSF performs exceptionally well, achieving the best performance on six out of the eight benchmarks and the second-best on the remaining two, highlighting its potential as a universal forecasting model.

After pre-training on  $\mathcal{D}_p$ , FlexTSF demonstrates effective performance by fine-tuning only the Leader node (a small subset of parameters) on target domains using varying numbers of samples drawn from the training sets of  $\mathcal{D}_h$ . Figure 4 presents the results. For reference, the best, median, and worst outcomes from full-shot training are also shown. FlexTSF consistently outperforms

**Table 3: Results (MSE) on irregular time series datasets with different forecast lengths.  $H/M$  indicates the ratio of forecasting horizon ( $H$ ) to input length ( $M$ ). The best results are in bold, and the second best are underlined.**

$H/M$	Regular					Irregular					Ours	
	DLinear	NHiTS	PatchTST	iTransformer	TimeMixer	mTAN	Latent-Flow	CRU	ContiFormer	IVP-VAE	t-PatchGNN	FlexTSF
SaTSM	0.25	0.294±0.001	0.488±0.002	0.277±0.007	0.270±0.003	0.278±0.003	0.345±0.053	0.568±0.038	<b>0.262±0.003</b>	0.440±0.055	0.394±0.035	0.347±0.018
	0.50	0.372±0.001	0.498±0.002	0.354±0.001	0.341±0.001	0.355±0.000	0.385±0.021	0.502±0.013	<u>0.338±0.002</u>	0.449±0.013	0.423±0.004	0.411±0.005
	1.00	0.424±0.000	0.546±0.003	0.363±0.001	<b>0.353±0.001</b>	0.375±0.001	0.448±0.004	0.542±0.038	0.375±0.006	0.547±0.028	0.519±0.004	0.481±0.004
MetrlA	0.25	0.365±0.000	1.051±0.002	0.356±0.001	<u>0.345±0.001</u>	0.352±0.000	0.400±0.002	0.403±0.014	0.392±0.000	0.384±0.001	0.415±0.002	0.422±0.009
	0.50	0.448±0.000	1.041±0.001	0.450±0.000	<u>0.428±0.000</u>	0.443±0.001	0.435±0.002	0.452±0.009	0.433±0.001	0.436±0.002	0.449±0.002	0.472±0.012
	1.00	0.571±0.000	1.049±0.001	0.601±0.000	0.542±0.001	0.590±0.001	0.498±0.007	0.630±0.027	<u>0.491±0.003</u>	0.612±0.005	0.498±0.005	0.513±0.019
ArabDigit	0.25	0.825±0.000	0.925±0.001	0.730±0.002	0.617±0.002	0.732±0.016	0.568±0.028	<b>0.543±0.002</b>	0.553±0.004	0.546±0.010	0.550±0.003	0.759±0.017
	0.50	0.928±0.001	0.963±0.002	0.865±0.003	0.732±0.003	0.856±0.009	0.677±0.002	0.676±0.005	0.678±0.007	0.683±0.015	<u>0.674±0.004</u>	0.825±0.025
	1.00	0.905±0.001	0.912±0.003	0.872±0.003	0.753±0.003	0.854±0.003	0.720±0.018	<u>0.712±0.003</u>	0.725±0.010	0.741±0.009	0.728±0.004	0.974±0.018
CharTraj	0.25	0.479±0.001	0.262±0.009	0.318±0.008	0.172±0.009	0.372±0.008	0.347±0.004	0.383±0.059	0.210±0.007	0.298±0.034	<u>0.160±0.002</u>	0.553±0.013
	0.50	0.615±0.001	0.399±0.000	0.440±0.004	0.257±0.010	0.483±0.008	0.476±0.010	<u>0.250±0.012</u>	0.463±0.017	0.516±0.044	0.305±0.006	0.716±0.026
	1.00	0.773±0.003	0.403±0.006	0.454±0.009	0.319±0.009	0.552±0.015	0.586±0.015	<u>0.300±0.001</u>	0.636±0.009	0.644±0.024	0.394±0.004	0.809±0.020
HAR	0.25	0.621±0.066	0.934±0.009	0.252±0.020	0.227±0.026	0.478±0.035	0.298±0.016	0.350±0.010	0.463±0.009	0.443±0.021	0.222±0.012	<u>0.202±0.023</u>
	0.50	0.678±0.018	0.930±0.003	0.285±0.017	0.241±0.030	0.568±0.026	0.307±0.011	0.342±0.001	0.517±0.014	0.450±0.010	0.247±0.012	<u>0.239±0.018</u>
	1.00	0.686±0.027	0.813±0.006	0.311±0.004	<u>0.256±0.009</u>	0.630±0.020	0.323±0.015	0.343±0.003	0.643±0.011	0.453±0.013	0.275±0.011	0.259±0.017
elCU	0.25	0.658±0.008	0.976±0.029	0.581±0.012	0.564±0.013	0.557±0.017	0.482±0.015	0.620±0.055	0.557±0.016	0.859±0.049	0.716±0.020	0.781±0.016
	0.50	0.671±0.005	0.951±0.020	0.610±0.003	0.595±0.009	0.590±0.014	<u>0.530±0.011</u>	0.582±0.028	0.621±0.025	0.865±0.025	0.615±0.016	0.819±0.051
	1.00	0.714±0.007	0.938±0.011	0.669±0.005	0.658±0.005	0.647±0.006	0.600±0.008	0.626±0.052	0.726±0.015	0.868±0.005	0.752±0.090	0.875±0.044
Physio12	0.25	0.563±0.042	0.855±0.053	0.546±0.043	0.520±0.034	0.489±0.040	<u>0.457±0.047</u>	0.646±0.000	0.530±0.049	0.758±0.025	0.543±0.043	0.632±0.042
	0.50	0.599±0.042	0.867±0.052	0.587±0.046	0.557±0.037	0.527±0.042	<u>0.500±0.043</u>	0.772±0.104	0.581±0.049	0.762±0.029	0.593±0.045	0.705±0.048
	1.00	0.622±0.028	0.862±0.038	0.607±0.026	0.589±0.018	0.561±0.031	<u>0.532±0.030</u>	0.810±0.109	0.608±0.025	0.764±0.019	0.774±0.018	0.765±0.015
MIMIC4	0.25	0.733±0.002	0.906±0.009	0.661±0.015	0.686±0.005	0.635±0.006	<u>0.593±0.017</u>	0.909±0.078	0.672±0.012	0.933±0.008	0.865±0.040	0.901±0.065
	0.50	0.752±0.017	0.903±0.009	0.693±0.007	0.709±0.010	0.669±0.018	<u>0.635±0.003</u>	0.965±0.094	0.720±0.005	0.915±0.001	0.899±0.068	0.925±0.070
	1.00	0.802±0.015	0.924±0.004	0.752±0.010	0.764±0.010	0.725±0.016	<u>0.706±0.014</u>	0.973±0.141	0.783±0.019	0.920±0.000	0.967±0.080	0.967±0.085

**Figure 3: Test MSE of four representative models under varying missing rates. A missing rate of 0% indicates fully observed regular time series.****Figure 4: Results of the low-resource fine-tuning experiments. The x-axis shows the number of samples used for fine-tuning. The best, median, and worst full-shot training results from Section 5.2 are shown on the plots for reference.**

**Table 4: Zero-shot forecasting performance comparison between FlexTSF and other pre-trained models on irregular time series datasets. Best in bold, second best underlined.**

Dataset	Lag-Llama	TimesFM	MOIRAI-MoE	Sundial	ARIMA	FlexTSF
SaTSM	0.946	0.900	0.913	<u>0.684</u>	0.895	<b>0.675</b>
MetrLA	0.691	0.645	0.563	<u>0.365</u>	0.771	0.420
ArabDigit	0.947	1.038	1.076	<u>0.767</u>	0.943	0.881
CharTraj	<u>0.513</u>	0.908	0.637	0.541	0.619	<b>0.414</b>
HAR	0.464	0.681	<u>0.350</u>	0.550	0.685	<b>0.242</b>
eICU	0.710	0.915	0.878	<u>0.604</u>	0.944	<b>0.593</b>
Physio12	0.747	1.052	0.795	<u>0.515</u>	0.834	<b>0.492</b>
MIMIC4	0.725	0.930	0.893	<u>0.687</u>	0.918	<b>0.608</b>

the worst full-shot results, exceeds the median on five datasets, and matches the best on two. This capability reduces the time and computational resources required for domain adaptation, making it effective in scenarios with limited training data.

#### 5.4 Ablation Study & Patch Length

*Impact of Components.* To assess the contribution of each component—IVP Patcher, time normalization, and the Leader node—we conduct an ablation study by independently removing one component at a time. Table 5 presents the MSE changes relative to the original FlexTSF model in zero-shot scenarios. The performance degradations demonstrate the effectiveness of these components.

**Table 5: Ablation results for FlexTSF. MSE+/- indicates the change relative to FlexTSF’s zero-shot results in Table 4.**

Dataset	IVP Patcher		Time Norm		Leader Node	
	MSE	MSE+/-	MSE	MSE+/-	MSE	MSE+/-
SaTSM	0.703	+4.15%	0.676	+0.15%	0.688	+1.93%
MetrLA	0.459	+9.29%	0.486	+15.71%	0.466	+10.95%
ArabDigit	0.908	+3.06%	0.888	+0.79%	0.944	+7.15%
CharTraj	0.544	+31.40%	0.535	+29.23%	0.519	+25.36%
HAR	0.291	+20.25%	0.245	+1.24%	0.248	+2.48%
eICU	0.630	+6.24%	0.652	+9.95%	0.614	+3.54%
Physio12	0.548	+11.38%	0.528	+7.32%	0.500	+1.63%
MIMIC4	0.626	+2.96%	0.652	+7.24%	0.638	+4.93%
Average	0.589	+11.09%	0.583	+8.95%	0.577	+7.25%

*Impact of Random Patch Lengths.* To investigate the impact of the random patch length strategy (Section 4.2.4), Figure 5 compares models trained with random patch lengths (FlexTSF-R) and deterministic patch lengths (FlexTSF-D). Across all datasets and  $H/M$  values (0.25, 0.50, 1.00), FlexTSF-R consistently achieves lower test MSE than FlexTSF-D. The performance gap becomes especially pronounced when the forecast length is larger (i.e.,  $H/M = 1.00$ ), highlighting the advantage of randomization and multi-patch composition in capturing long-term temporal patterns.

To better understand how the model dynamically utilizes different patch lengths, Figure 6 shows a heatmap of the average attention weight assigned to each patch length across datasets and forecast ratios by FlexTSF-R, averaged over multiple random seeds. The

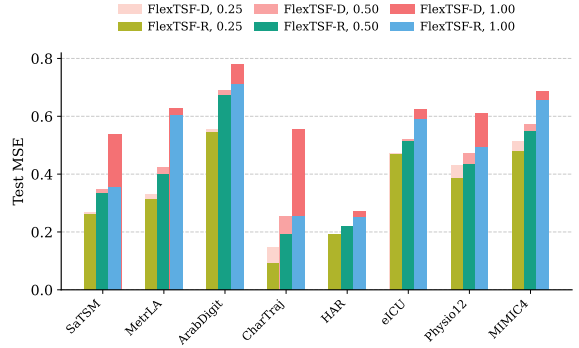


**Figure 5: Comparison of models trained by random patch lengths (FlexTSF-R) and deterministic patch lengths (FlexTSF-D) across different  $H/M$  values (0.25, 0.50, 1.00).**

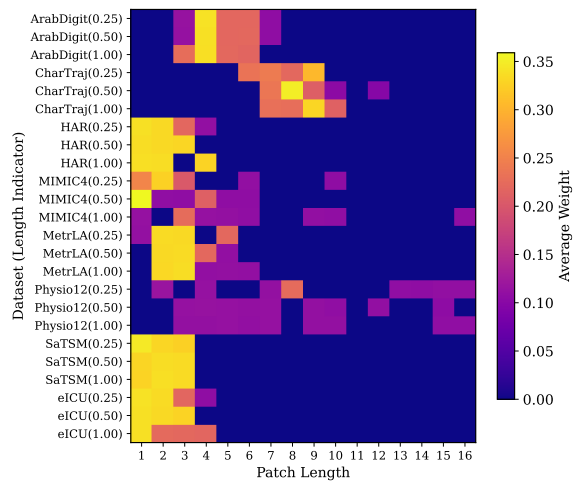


**Figure 6: Patch length distribution after dynamic selection. Each row corresponds to a dataset and forecast-ratio setting.**

distribution varies significantly depending on the dataset and  $H/M$  value, indicating that FlexTSF-R adaptively emphasizes different patch lengths based on task characteristics.

## 6 Conclusion

We have presented FlexTSF, a flexible forecasting model designed to handle time series data with diverse and irregular temporal characteristics. By introducing the IVP Patcher, FlexTSF overcomes the limitations of fixed-window patching and learns continuous-time latent dynamics capable of handling arbitrary sampling intervals and missing values. Our time normalization strategy, combined with the Leader node, enables domain self-adaptation by decoupling static domain information extraction from temporal pattern learning. The use of random patch lengths further enhances FlexTSF’s flexibility, reducing manual tuning and improving performance in modeling long-term dependencies.

Future work includes improving the efficiency of the IVP Patcher by exploring faster IVP solvers, extending the current channel-independent framework to fully multivariate inputs, developing adaptive patch length sampling strategies (e.g., via reinforcement learning), and pre-training on larger datasets to clarify the relationship between data scale and generalization.

## References

- [1] Abdul Fatir Ansari, Lorenzo Stella, Caner Turkmen, Xiyuan Zhang, Pedro Mercado, Huibin Shen, Oleksandr Shchur, Syama Sundar Rangapuram, Sebastian Pineda Arango, Shubham Kapoor, et al. 2024. Chronos: Learning the Language of Time Series. *Transactions on Machine Learning Research* 2024 (2024).
- [2] Anthony Bagnall, Hoang Anh Dau, Jason Lines, Michael Flynn, James Large, Aaron Bostrom, Paul Southam, and Eamonn Keogh. 2018. The UEA multivariate time series classification archive, 2018. *arXiv preprint arXiv:1811.00075* (2018).
- [3] Tony Bagnall. 2024. Time Series Classification Website. <https://www.timeseriesclassification.com/index.php>. Accessed: 2024-03-03.
- [4] Marin Biloš, Johanna Sommer, Syama Sundar Rangapuram, Tim Januschowski, and Stephan Günnemann. 2021. Neural Flows: Efficient Alternative to Neural ODEs. In *Advances in Neural Information Processing Systems*, Vol. 34. Curran Associates, Inc., 21325–21337.
- [5] Tim Bollerslev. 1986. Generalized autoregressive conditional heteroskedasticity. *Journal of econometrics* 31, 3 (1986), 307–327.
- [6] Anastasia Borovykh, Sander Bohte, and Cornelis W Oosterlee. 2018. Dilated convolutional neural networks for time series forecasting. *Journal of Computational Finance, Forthcoming* (2018).
- [7] G.E.P. Box and G.M. Jenkins. 1970. *Time Series Analysis: Forecasting and Control*. Holden-Day.
- [8] Defu Cao, Furong Jia, Sercan O Arik, Tomas Pfister, Yixiang Zheng, Wen Ye, and Yan Liu. 2024. TEMPO: Prompt-based Generative Pre-trained Transformer for Time Series Forecasting. In *The 12th International Conference on Learning Representations*.
- [9] Cristian Challu, Kin G Olivares, Boris N Oreshkin, Federico Garza Ramirez, Max Mergenthaler Canseco, and Artur Dubrawski. 2023. NHITS: Neural Hierarchical Interpolation for Time Series Forecasting. In *Proceedings of the AAAI Conference on Artificial Intelligence*, Vol. 37. 6989–6997.
- [10] Zhengping Che, Sanjay Purushotham, Kyunghyun Cho, David Sontag, and Yan Liu. 2018. Recurrent Neural Networks for Multivariate Time Series with Missing Values. *Scientific Reports* 8 (2018), 1–12. Issue 1.
- [11] Jialin Chen, Aosong Feng, Ziyu Zhao, Juan Garza, Gaukhar Nurbek, Cheng Qin, Ali Maatouk, Leandros Tassiulas, Yifeng Gao, and Rex Ying. 2025. Mtbench: A multimodal time series benchmark for temporal reasoning and question answering. *arXiv preprint arXiv:2503.16858* (2025).
- [12] Ricky T. Q. Chen, Yulia Rubanova, Jesse Bettencourt, and David K Duvenaud. 2018. Neural Ordinary Differential Equations. In *Advances in Neural Information Processing Systems*, Vol. 31. Curran Associates, Inc.
- [13] Yuqi Chen, Kan Ren, Yansen Wang, Yuchen Fang, Weiwei Sun, and Dongsheng Li. 2023. ContiFormer: Continuous-time transformer for irregular time series modeling. In *Advances in Neural Information Processing Systems*.
- [14] Luke Nicholas Darlow, Qiwen Deng, Ahmed Hassan, Martin Asenov, Rajkarn Singh, Artjom Joosen, Adam Barker, and Amos Storkey. 2024. DAM: Towards a Foundation Model for Forecasting. In *The 12th International Conference on Learning Representations*.
- [15] Abhimanyu Das, Weihao Kong, Rajat Sen, and Yichen Zhou. 2024. A Decoder-only Foundation Model for Time-series Forecasting. In *The 41st International Conference on Machine Learning*.
- [16] Hoang Anh Dau, Anthony Bagnall, Kaveh Kamgar, Chin-Chia Michael Yeh, Yan Zhu, Shaghayegh Gharghabi, Chotirat Ann Ratanamahatana, and Eamonn Keogh. 2019. The UCR time series archive. *IEEE/CAA Journal of Automatica Sinica* 6, 6 (2019), 1293–1305.
- [17] Jan G De Gooijer and Rob J Hyndman. 2006. 25 years of time series forecasting. *International journal of forecasting* 22, 3 (2006), 443–473.
- [18] Samuel Dooley, Gurnoor Singh Khurana, Chirag Mohapatra, Siddartha V Naidu, and Colin White. 2024. ForecastPFN: Synthetically-trained zero-shot forecasting. In *Advances in Neural Information Processing Systems*, Vol. 36.
- [19] Alexey Dosovitskiy. 2020. An image is worth 16x16 words: Transformers for image recognition at scale. *arXiv preprint arXiv:2010.11929* (2020).
- [20] Rakshitha Godahewa, Christoph Bergmeir, Geoffrey I. Webb, Rob J. Hyndman, and Pablo Montero-Manso. 2021. Monash Time Series Forecasting Archive. In *Neural Information Processing Systems Track on Datasets and Benchmarks*.
- [21] Ming Jin, Shiyu Wang, Lintao Ma, Zhixuan Chu, James Y Zhang, Xiaoming Shi, Pin-Yu Chen, Yuxuan Liang, Yuan-Fang Li, Shirui Pan, et al. 2024. Time-LLM: Time Series Forecasting by Reprogramming Large Language Models. In *The 12th International Conference on Learning Representations*.
- [22] Dongbin Kim, Jinseong Park, Jaewook Lee, and Hoki Kim. 2024. Are Self-Attentions Effective for Time Series Forecasting?. In *The Thirty-eighth Annual Conference on Neural Information Processing Systems*.
- [23] Diederik P. Kingma and Max Welling. 2014. Auto-Encoding Variational Bayes. In *International Conference on Learning Representations (ICLR)*.
- [24] Yaxuan Kong, Yiyuan Yang, Yoontae Hwang, Wenjie Du, Stefan Zohren, Zhangyang Wang, Ming Jin, and Qingsong Wen. 2025. Time-MQA: Time Series Multi-Task Question Answering with Context Enhancement. In *Proceedings of the 63rd Annual Meeting of the Association for Computational Linguistics (Long Papers)*. 29736–29753.
- [25] Guokun Lai, Wei-Cheng Chang, Yiming Yang, and Hanxiao Liu. 2018. Modeling long-and short-term temporal patterns with deep neural networks. In *The 41st international ACM SIGIR conference on research & development in information retrieval*. 95–104.
- [26] Shiyang Li, Xiaoyong Jin, Yao Xuan, Xiyou Zhou, Wenhui Chen, Yu-Xiang Wang, and Xifeng Yan. 2019. Enhancing the Locality and Breaking the Memory Bottleneck of Transformer on Time Series Forecasting. In *Advances in Neural Information Processing Systems*, Vol. 32. Curran Associates, Inc.
- [27] Yaguang Li, Rose Yu, Cyrus Shahabi, and Yan Liu. 2018. Diffusion Convolutional Recurrent Neural Network: Data-Driven Traffic Forecasting. In *International Conference on Learning Representations*.
- [28] Bryan Lim and Stefan Zohren. 2021. Time-series forecasting with deep learning: a survey. *Philosophical Transactions of the Royal Society A* 379, 2194 (2021), 20200209.
- [29] Shizhan Liu, Hang Yu, Cong Liao, Jianguo Li, Weiyao Lin, Alex X Liu, and Schahram Dusdar. 2021. Pyraformer: Low-complexity pyramidal attention for long-range time series modeling and forecasting. In *International conference on learning representations*.
- [30] Xu Liu, Juncheng Liu, Gerald Woo, Taha Aksu, Yuxuan Liang, Roger Zimmermann, Chenghao Liu, Junnan Li, Silvio Savarese, Caiming Xiong, and Doyen Sahoo. 2025. Moirai-MoE: Empowering Time Series Foundation Models with Sparse Mixture of Experts. In *Forty-second International Conference on Machine Learning*.
- [31] Yong Liu, Tengge Hu, Haoran Zhang, Haixu Wu, Shiyu Wang, Lintao Ma, and Mingsheng Long. 2024. iTransformer: Inverted Transformers Are Effective for Time Series Forecasting. In *The Twelfth International Conference on Learning Representations*.
- [32] Yong Liu, Guo Qin, Xiangdong Huang, Jianmin Wang, and Mingsheng Long. 2025. Timer-XL: Long-Context Transformers for Unified Time Series Forecasting. In *The Thirteenth International Conference on Learning Representations*.
- [33] Yong Liu, Guo Qin, Zhiyuan Shi, Zhi Chen, Caiyin Yang, Xiangdong Huang, Jianmin Wang, and Mingsheng Long. 2025. Sundial: A Family of Highly Capable Time Series Foundation Models. In *Forty-second International Conference on Machine Learning*.
- [34] Donghao Luo and Xue Wang. 2024. DeformableTST: Transformer for Time Series Forecasting without Over-reliance on Patching. In *The Thirty-eighth Annual Conference on Neural Information Processing Systems*.
- [35] Yuqi Nie, Nam H Nguyen, Phanwadee Sinthong, and Jayant Kalagnanam. 2023. A Time Series is Worth 64 Words: Long-term Forecasting with Transformers. In *The 11th International Conference on Learning Representations*.
- [36] Alec Radford, Jeffrey Wu, Rewon Child, David Luan, Dario Amodei, Ilya Sutskever, et al. 2019. Language models are unsupervised multitask learners. *OpenAI blog* 1, 8 (2019), 9.
- [37] Colin Raffel, Noam Shazeer, Adam Roberts, Katherine Lee, Sharan Narang, Michael Matena, Yanqi Zhou, Wei Li, and Peter J Liu. 2020. Exploring the limits of transfer learning with a unified text-to-text transformer. *Journal of machine learning research* 21, 140 (2020), 1–67.
- [38] Kashif Rasul, Arjun Ashok, Andrew Robert Williams, Arian Khorasani, George Adamopoulos, Rishika Bhagwatkar, Marin Biloš, Hena Ghonia, Nadhir Vincent Hassen, Anderson Schneider, et al. 2023. Lag-Llama: Towards foundation models for time series forecasting. *arXiv preprint arXiv:2310.08278* (2023).
- [39] Yulia Rubanova, Ricky TQ Chen, and David K Duvenaud. 2019. Latent ordinary differential equations for irregularly-sampled time series. In *Advances in neural information processing systems*, Vol. 32.
- [40] David Salinas, Valentin Flunkert, Jan Gasthaus, and Tim Januschowski. 2020. DeepAR: Probabilistic forecasting with autoregressive recurrent networks. *International journal of forecasting* 36, 3 (2020), 1181–1191.
- [41] Timothy Sauer. 2012. *Numerical Analysis* (2 ed.). Pearson, Boston.
- [42] Mona Schirmer, Mazin Eltayeb, Stefan Lessmann, and Maja Rudolph. 2022. Modeling irregular time series with continuous recurrent units. In *International conference on machine learning*. PMLR, 19388–19405.
- [43] Xiaoming Shi, Shiyu Wang, Yuqi Nie, Dianqi Li, Zhou Ye, Qingsong Wen, and Ming Jin. 2025. Time-MoE: Billion-Scale Time Series Foundation Models with Mixture of Experts. In *The Thirteenth International Conference on Learning Representations*.
- [44] Satya Narayan Shukla and Benjamin M. Marlin. 2021. Multi-Time Attention Networks for Irregularly Sampled Time Series. In *International Conference on Learning Representations (ICLR)*.

[45] Jianlin Su, Murtadha Ahmed, Yu Lu, Shengfeng Pan, Wen Bo, and Yunfeng Liu. 2024. RoFormer: Enhanced transformer with rotary position embedding. *Neurocomputing* 568 (2024), 127063.

[46] Chenxi Sun, Yaliang Li, Hongyan Li, and Shenda Hong. 2024. TEST: Text prototype aligned embedding to activate LLM's ability for time series. In *The 12th International Conference on Learning Representations*.

[47] Mingtian Tan, Mike Merrill, Vinayak Gupta, Tim Althoff, and Tom Hartvigsen. 2024. Are language models actually useful for time series forecasting? *Advances in Neural Information Processing Systems* 37 (2024), 60162–60191.

[48] Chengsen Wang, Qi Qi, Jingyu Wang, Haifeng Sun, Zirui Zhuang, Jinming Wu, Lei Zhang, and Jianxin Liao. 2025. Chattime: A unified multimodal time series foundation model bridging numerical and textual data. In *Proceedings of the AAAI Conference on Artificial Intelligence*, Vol. 39. 12694–12702.

[49] Shiyu Wang, Haixu Wu, Xiaoming Shi, Tengge Hu, Huakun Luo, Lintao Ma, James Y. Zhang, and JUN ZHOU. 2024. TimeMixer: Decomposable Multiscale Mixing for Time Series Forecasting. In *The Twelfth International Conference on Learning Representations*.

[50] Yuxuan Wang, Haixu Wu, Jiaxiang Dong, Guo Qin, Haoran Zhang, Yong Liu, Yunzhong Qiu, Jianmin Wang, and Mingsheng Long. 2024. TimeXer: Empowering Transformers for Time Series Forecasting with Exogenous Variables. In *The Thirty-eighth Annual Conference on Neural Information Processing Systems*.

[51] Philip B Weerakody, Kok Wai Wong, Guanjin Wang, and Wendell Ela. 2021. A Review of Irregular Time Series Data Handling with Gated Recurrent Neural Networks. *Neurocomputing* 441 (2021), 161–178.

[52] Gerald Woo, Chenghao Liu, Akshat Kumar, Caiming Xiong, Silvio Savarese, and Doyen Sahoo. 2024. Unified Training of Universal Time Series Forecasting Transformers. In *The 41st International Conference on Machine Learning*.

[53] Haixi Wu, Jiehui Xu, Jianmin Wang, and Mingsheng Long. 2021. Autoformer: Decomposition Transformers with Auto-Correlation for Long-Term Series Forecasting. In *Advances in Neural Information Processing Systems*, Vol. 34. Curran Associates, Inc., 22419–22430.

[54] Jingge Xiao, Leonie Basso, Wolfgang Nejdl, Niloy Ganguly, and Sandipan Sikdar. 2024. IVP-VAE: Modeling EHR Time Series with Initial Value Problem Solvers. In *Proceedings of the AAAI Conference on Artificial Intelligence*, Vol. 38. 16023–16031.

[55] Zhe Xie, Zeyan Li, Xiao He, Longlong Xu, Xida Wen, Tieying Zhang, Jianjun Chen, Rui Shi, and Dan Pei. 2024. ChatTS: Aligning Time Series with LLMs via Synthetic Data for Enhanced Understanding and Reasoning. *arXiv preprint arXiv:2412.03104* (2024).

[56] Hao Xue and Flora D Salim. 2023. PromptCast: A new prompt-based learning paradigm for time series forecasting. *IEEE Transactions on Knowledge and Data Engineering* (2023).

[57] Jiexia Ye, Weiqi Zhang, Ke Yi, Yongzi Yu, Ziyue Li, Jia Li, and Fugee Tsung. 2024. A Survey of Time Series Foundation Models: Generalizing Time Series Representation with Large Language Model. *arXiv preprint arXiv:2405.02358* (2024).

[58] Ailing Zeng, Muxi Chen, Lei Zhang, and Qiang Xu. 2023. Are transformers effective for time series forecasting? In *Proceedings of the AAAI conference on artificial intelligence*, Vol. 37. 11121–11128.

[59] Weijia Zhang, Chenlong Yin, Hao Liu, Xiaofang Zhou, and Hui Xiong. 2024. Irregular Multivariate Time Series Forecasting: A Transformable Patching Graph Neural Networks Approach. In *Forty-first International Conference on Machine Learning*.

[60] Yunhao Zhang and Junchi Yan. 2023. Crossformer: Transformer Utilizing Cross-Dimension Dependency for Multivariate Time Series Forecasting. In *The Eleventh International Conference on Learning Representations*. <https://openreview.net/forum?id=vSVLM2j9eie>

[61] Haoyi Zhou, Shanghang Zhang, Jieqi Peng, Shuai Zhang, Jianxin Li, Hui Xiong, and Wancai Zhang. 2021. Informer: Beyond efficient transformer for long sequence time-series forecasting. In *Proceedings of the AAAI conference on artificial intelligence*, Vol. 35. 11106–11115.

[62] Tian Zhou, Ziqing Ma, Qingsong Wen, Xue Wang, Liang Sun, and Rong Jin. 2022. FEDformer: Frequency enhanced decomposed transformer for long-term series forecasting. In *International conference on machine learning*. PMLR, 27268–27286.

[63] Tian Zhou, Peisong Niu, Xue Wang, Liang Sun, and Rong Jin. 2023. One Fits All: Power General Time Series Analysis by Pretrained LM. In *Conference on Neural Information Processing Systems*.

## A Appendix

### A.1 More Related Works

**A.1.1 Transformers for Time Series Forecasting.** Time series forecasting has evolved from classical statistical methods such as ARIMA [7] and GARCH [5] to deep learning models based on RNNs [40], CNNs [6], and more recently, Transformers [61]. Their success in NLP has inspired adaptations for time series, where modeling long-range dependencies and variable interactions is crucial. Early Transformer-based models for time series forecasting, including LogTrans [26], Informer [61], Autoformer [53], FEDformer [62], and Pyraformer [29], introduced various architectural innovations to reduce the quadratic complexity of self-attention and improve long-horizon forecasting. These include mechanisms like convolutional or ProbSparse attention, trend-seasonality decomposition, and frequency-domain transforms.

A major turning point came with PatchTST [35], which replaces tokenization at individual timestamps with fixed-length temporal patches. This design captures local temporal patterns more robustly and, combined with instance normalization, has become a strong baseline for both univariate and multivariate forecasting. Recent models extend this line of work in various ways. Crossformer [60] uses a two-stage attention mechanism alternating between temporal and inter-variable dimensions to model multivariate interactions. iTransformer [31] treats variables as tokens and time as channels, shifting attention to cross-variable patterns while using feed-forward layers for temporal modeling. ContiFormer [13] incorporates neural ODEs to enable continuous-time modeling of irregular time series.

**A.1.2 Universal Time Series Forecasting Model.** Recent universal forecasting models extend the Transformer lineage, using earlier design lessons as building blocks while aiming for broad zero-shot generalization instead of dataset-specific optimization. ForecastPFN [18] and DAM [14] use pointwise time-value pairs as input tokens within encoder-only models, but differ in their forecasting approaches: the former relies on time queries while the latter utilizes basis function composition. Lag-Llama [38] and TimesFM [15] employ decoder-only models, adopting autoregressive prediction, which is similar to next token prediction in LLMs, for training on time series data. MOIRAI [52] utilizes time series patches with multiple variables and leverages an encoder-only model trained via masked patch prediction. Its successor, MOIRAI-MoE [30], extends this architecture by incorporating a sparse Mixture-of-Experts (MoE) framework, which replaces the fixed frequency-based specialization with an adaptive token-level specialization. Timer-XL [32], a decoder-only Transformer, generalizes next-token prediction to multivariate next-token prediction and uses a universal TimeAttention mechanism to capture fine-grained dependencies between and within series of flattened time-series patches. Sundial [33] is a family of decoder-only Transformer models that are pre-trained on continuous-valued time series without discrete tokenization, using a TimeFlow loss based on flow-matching to generate multiple probable predictions. Among these models, FlexTSF stands out because of its native support for missing data, variable sequence lengths, and irregular time intervals, making it well-suited for diverse applications.

**A.1.3 LLM-based Forecasting Models.** Building on the success of LLMs across various domains, several studies have explored their adaptation to time series forecasting. PromptCast [56] reformulates numerical input as prompts, framing forecasting as a conversational task. GPT4TS [63] and Chronos [1] fine-tune GPT-2 [36] and T5 [37] directly on time series data or use specialized tokenization. Time-LLM [21] reprograms time series as prefix prompts based on text prototypes to enhance LLM reasoning. TEMPO [8] decomposes time series into trend, seasonal, and residual components to design distribution-adaptive prompts. TEST [46] applies contrastive learning to align time series with the LLM’s language space. However, a contemporary work [47] questions the utility of LLMs for forecasting, showing that removing the LLM or replacing it with a basic attention layer does not degrade performance, and that pretrained LLMs often underperform time series models trained from scratch. Recently, the focus has shifted towards multimodal reasoning that combines time series with natural language. ChatTime [48] treats time series as a foreign language to enable bi-modal forecasting and explanation. ChatTS [55] improves time series–LLM alignment using synthetic paired data. MTBench [11] provides a benchmark for evaluating temporal reasoning with multimodal QA tasks. Time-MQA [24] frames various time series tasks as QA and boosts LLM performance through continued pretraining on a large TSQA corpus. Since these methods focus on different problem settings, we did not include them as baselines for evaluating universal time series forecasting.

### A.2 Notations

An overview of notations used in this paper is given in Table 6.

### A.3 Additional Details of the Attention Module

We denote  $A$  as the intermediate representation passed through the attention blocks. The input to the first attention layer, denoted by  $A_0$ , is constructed as  $A_0 = [A_0^L, A_0^E, A_0^D]$ , where the concatenation is performed along the temporal axis. Here,  $A_0^L$  represents static domain features projected into the sequence space via the Leader node;  $A_0^E = \{r_k\}_{k=1}^K$  is the sequence of patch-level embeddings obtained from the encoder, where  $K$  is the number of input patches; and  $A_0^D$  denotes a set of learnable dummy patch representations corresponding to the forecast targets. This construction allows the attention layers to jointly reason over contextual, dynamic, and target information in a temporally coherent manner.

The input  $A_0$  is then passed through a stack of  $m$  decoder-style attention blocks, each equipped with layer-wise rotary time embeddings to inject temporal structure throughout the stack. Each attention layer employs a masking mechanism to enforce autoregressive ordering and to ensure that dummy patches remain independent of each other. After the final layer, the representations at the dummy patch positions, denoted by  $\hat{r} = A_m^D$ , are extracted and forwarded to the IVP Patcher for forecast generation. Beyond these components, the model adheres to a decoder-only causal self-attention architecture.

### A.4 Illustration of The Training Process

Figure 7 shows a simplified illustration of the training process. Let’s assume we have one variable in the time series, the patch length

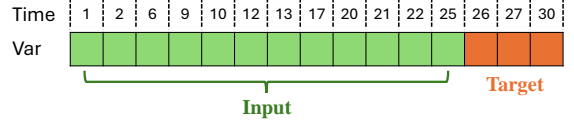
**Table 6: Notation used throughout the paper.**

Notation	Description
<i>Sequences and sets</i>	
$S$	A time series sample $\{(\mathbf{x}_i, t_i)\}_{i=1}^M$
$M$	Number of observations in $S$
$H$	Forecast horizon (number of future steps)
$\mathbf{x}_i$	Observation vector recorded at $t_i$
$\mathbf{X}$	Raw value sequence $\{\mathbf{x}_i\}_{i=1}^M$
$\mathbf{X}'$	Normalized values; $\mathbf{X}' = G_t(G_g(\mathbf{X}))$
$\mathbf{X}^+$	Future (ground-truth) values $\{\mathbf{x}_i\}_{i=M+1}^{M+H}$
$\mathbf{X}^*$	Full sequence $\{\mathbf{x}_i\}_{i=1}^{M+H}$
$T$	Raw timestamps $\{t_i\}_{i=1}^M$
$T'$	Normalized timestamps $\{t'_i\}_{i=1}^M$ (min. interval = 1)
<i>Normalisation statistics</i>	
$\mu_g, \sigma_g$	Dataset-level mean and standard deviation
$\mu_i, \sigma_i$	Instance-level mean and standard deviation
$\omega_g$	Dataset time unit (reciprocal sampling freq.)
$\omega_i$	Instance time unit (minimum raw interval)
$L$	Static vector $[\mu_g, \sigma_g, \mu_i, \sigma_i, \omega_g, \omega_i]$
<i>Patching</i>	
$V$	A patch (sub-sequence) $\{(\mathbf{x}_i, t_i)\}_{i=p_s}^{p_e}$
$p_s, p_e$	Starting / ending indices of a patch
$p$	Patch length, $p = p_e - p_s + 1$
$K$	Number of patches per input sequence
$\tau$	Time indicator (first timestamp) of a patch
<i>Latent variables</i>	
$\mathbf{z}_i$	Initial latent mapped from $\mathbf{x}_i$
$\mathbf{z}_{0,i}$	Latent evolved backward to $\tau$
$\mathbf{r}$	Patch representation sampled from $q_\phi$
$\hat{\mathbf{r}}$	Predicted patch representation (after attention)
$\hat{\mathbf{x}}_i$	Predicted observation value
<i>Continuous dynamics</i>	
$f$	ODE derivative $\frac{d\mathbf{z}(t)}{dt} = f(t, \mathbf{z}(t))$
$\Delta t_i$	Time interval $t_{i+1} - t_i$
$\pi_i$	Mixing weight of Gaussian $i$ in $q_\phi$
$KL_i$	KL divergence of component $i$ to $\mathcal{N}(\mathbf{0}, \mathbf{I})$
<i>Models and parameters</i>	
$q_\phi(\mathbf{z}_0 V)$	Recognition (posterior) model
$p_\theta(V \mathbf{z}_0)$	Generation (likelihood) model
$\phi, \theta$	Parameters of recognition / generation models
<i>Losses and weights</i>	
$\mathcal{L}_{\text{patch}}$	Patch-level ELBO loss
$\mathcal{L}_{\text{forecast}}$	Forecast negative log-likelihood loss
$\mathcal{L}$	Overall training objective
$\beta$	Weight between reconstruction and KL in $\mathcal{L}_{\text{patch}}$
$\lambda$	Weight between patch and forecast losses in $\mathcal{L}$
$\sigma^2$	Fixed variance in Gaussian forecast likelihood
<i>Datasets</i>	
$D$	A dataset
$\mathcal{D}_h$	Held-out dataset group
$\mathcal{D}_p$	Pre-trained dataset group

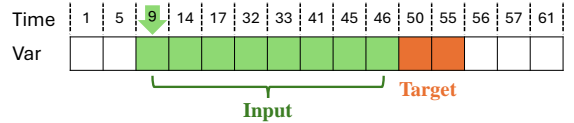
is 1, and observations are collected at irregular timestamps. In the supervised training or inference phase, each forward pass generates future patches in parallel. During unsupervised pre-training, instead of using the full sequence, a sub-sequence is randomly selected at each iteration. First, a starting position is randomly determined, followed by the random selection of the sub-sequence length. The goal of pre-training is to predict the observations that follow the sub-sequence.

## A.5 Hyperparameters and Model Settings

In this section, we detail the hyperparameters and configurations of FlexTSF used to produce the experimental results presented in



(a) Input and target during training &amp; inference



(b) Input and target during pre-training

**Figure 7: Input and target during training & inference, and pre-training.**

Section 5. These parameters are specified for each stage of the training process, including Classic Training, Pre-Training, and Fine-Tuning.

Parameter	Classic Training	Pre-Training	Fine-Tuning
Optimizer	Adam	AdamW	Adam
LR Scheduler	StepLR	CosineAnnealingLR	StepLR
Warmup-steps	–	1000	–
Batch size	64	64	64
Weight Decay	1e-4	0.1	1e-4
Learning Rate	1e-4	–	1e-4
LR Scheduler Step	20	–	20
LR Decay	0.5	–	0.5
beta1	–	0.9	–
beta2	–	0.95	–

**Table 7: Hyperparameters for Different Training Phases**

Parameter	Classic Training	Pre-Training, Zero-Shot, Fine-Tuning
Dimension of Each Head	16	64
Number of Heads	4	12
Number of Attention Layers	2	6
Dimension of IVP Solver	64	768
Total Parameters	440,066	61,488,514

**Table 8: FlexTSF Configuration for Different Training Modes**

## A.6 Dataset Details

Table 10 and Table 9 provide an overview of all datasets in  $\mathcal{D}_h$  and their characteristics. In Table 10, the "Min Time Unit" (in seconds) represents the smallest sampling interval in each dataset, corresponding to  $\omega_g$  as introduced in Section 4.3.

Table 9 presents summary statistics for the irregular time series datasets used in our experiments. For each dataset, we report the

**Table 9: Summary statistics of the irregular time series datasets**

<b>Dataset</b>	<b>Missing rate (%)</b>			<b>Input length</b>			<b>Time interval</b>		
	Min	Max	Mean	Min	Max	Mean	Min	Max	Mean
SaTSM	0.000	0.000	0.000	8	48	26	1.00	335.00	12.91
MetrLA	0.000	63.647	3.945	4	12	11	3.5e-3	3.5e-3	3.5e-3
ArabDigit	5.385	14.253	10.003	4	41	19	1.00	1.00	1.00
CharTraj	5.247	17.313	10.087	30	91	59	1.00	1.00	1.00
HAR	74.000	75.000	74.995	25	25	25	1.00	17.00	3.31
eICU	29.803	85.900	65.131	30	146	57	1.00	851.00	24.83
Physio12	74.079	92.174	84.203	4	85	37	1.00	1220.00	38.15
MIMIC-IV	96.109	98.502	97.895	50	330	110	1.00	856.00	12.73

minimum, maximum, and mean values of the missing rate, input sequence length, and time interval between consecutive observations. Since the temporal granularity of the datasets varies, we express the time intervals as multiples of the "Min Time Unit". While datasets like MetrLA, ArabDigit, and CharTraj exhibit varying sequence lengths and a moderate level of missing values, HAR combines a high missing rate with non-uniform time intervals. SaTSM has variable sequence lengths and irregular intervals. Notably, eICU, Physio12, and MIMIC-IV are particularly challenging due to their high missing rates, wide variation in sequence length, and irregular sampling intervals.

The original ArabDigit and CharTraj datasets mainly exhibit variable sequence lengths with only limited missingness. To increase the difficulty of model evaluation, we randomly dropped 10% of the observations in these datasets. As zero-shot models do not access the training or validation partitions, and both zero-shot and full-shot models are evaluated on the same test sets, all statistics reported in Table 9 are computed solely on the test partition of each dataset. The preprocessing scripts used to generate these statistics are available in the released codebase.

- ETT1, ETT2, ETTm1, ETTm2, ExRate, Illness, Weather, Electricity, URL: <https://github.com/thuml/Autoformer>
- SaTSM, URL: <https://zenodo.org/records/5712933>
- MetrLA (Full name: METR-LA), URL: <https://github.com/liyaguang/DCRNN>
- ArabDigit (Full name: SpokenArabicDigits), URL: <https://archive.ics.uci.edu/dataset/195/spoken+arabic+digit>
- CharTraj (Full name: CharacterTrajectories), URL: <https://archive.ics.uci.edu/dataset/175/character+trajectories>
- HAR, URL: <https://archive.ics.uci.edu/dataset/196/localization+data+for+person+activity>
- eICU, URL: <https://physionet.org/content/eicu-crd/2.0/>
- Physio12 (Full name: PhysioNet2012), URL: <https://physionet.org/content/challenge-2012/1.0.0/>
- MIMIC4 (Full name: MIMIC-IV), URL: <https://physionet.org/content/mimiciv/1.0/>

**Table 10: Characteristics of the datasets in  $\mathcal{D}_h$ .**

Dataset	Domain	# Variables	Min Time Unit (s)
ETT1	Power Systems	7	3600
ETT2	Power Systems	7	3600
ETTm1	Power Systems	7	900
ETTm2	Power Systems	7	900
ExRate	Finance	8	86400
Illness	Epidemiology	7	604800
Weather	Meteorology	21	600
Electricity	Electricity Consumption	321	3600
SaTSM	Earth Observation	13	86400
MetrLA	Traffic	207	86400
ArabDigit	Speech Recognition	13	0.000091
CharTraj	Handwriting Recognition	3	0.005
HAR	Human Activity Recognition	12	0.1
eICU	Healthcare	14	60
Physio12	Healthcare	37	60
MIMIC4	Healthcare	71	60

To maintain a clean layout in tables and figures, some dataset names are abbreviated. The full names and links to download the data are: